Astrophysical Phenomena Revealed by Space VLBI
H. Hirabayashi, P.G. Edwards and D.W. Murphy (eds.)

High Resolution X-Ray Imaging and Spectroscopy of AGN and SS 433 with the Chandra X-Ray Observatory

Herman L. Marshall

Center for Space Research, MIT, Cambridge, MA 02139, USA

Abstract

We present some early results on AGN and jets with the Chandra X-ray Observatory, highlighting high resolution spectroscopy using the High Energy Transmission Grating Spectrometer (HETGS). The quasar PKS 0637–752 was found to have a very bright X-ray jet whose shape is remarkably similar to that of the radio jet on a size scale of 100 kpc but the X-ray emission is still unexplainably bright. Two BL Lac objects, PKS 2155–304 and Mk 421, were observed with the spectrometer and found to have no strong absorption or emission features. Other radio loud AGN observed with the HETGS show simple power law spectra without obvious features. These AGN results stand in marked contrast to the line-rich spectrum of SS 433, a Galactic X-ray binary which has relativistic jets. Broadened X-ray emission lines of H- and He-like S and Si are used to show that the characteristic temperature of the jet is near 2.5 keV at its base.

1 Introduction

The Chandra X-ray Observatory (CXO, or Chandra) was launched in July, 1999 into high Earth orbit. Although there has been some degradation of the spectral resolution of the Advanced CCD Imaging Spectrometer (ACIS), all instruments are performing extremely well.

The main scientific feature of Chandra is the mirror performance: the half-power radius is about $0.4''$. In addition, there are two objective grating spectrometers, providing a spectral resolution, E/dE, of 200–2000 in the 0.1–10 keV range. The ACIS detector provides $\sim$ 100 eV resolution over the energy range from 0.5-10 keV and the High Resolution Camera gives higher timing resolution and the best spatial resolution.

We will focus on data from ACIS and the HETGS here in order to demonstrate the overall performance of the telescope and some of

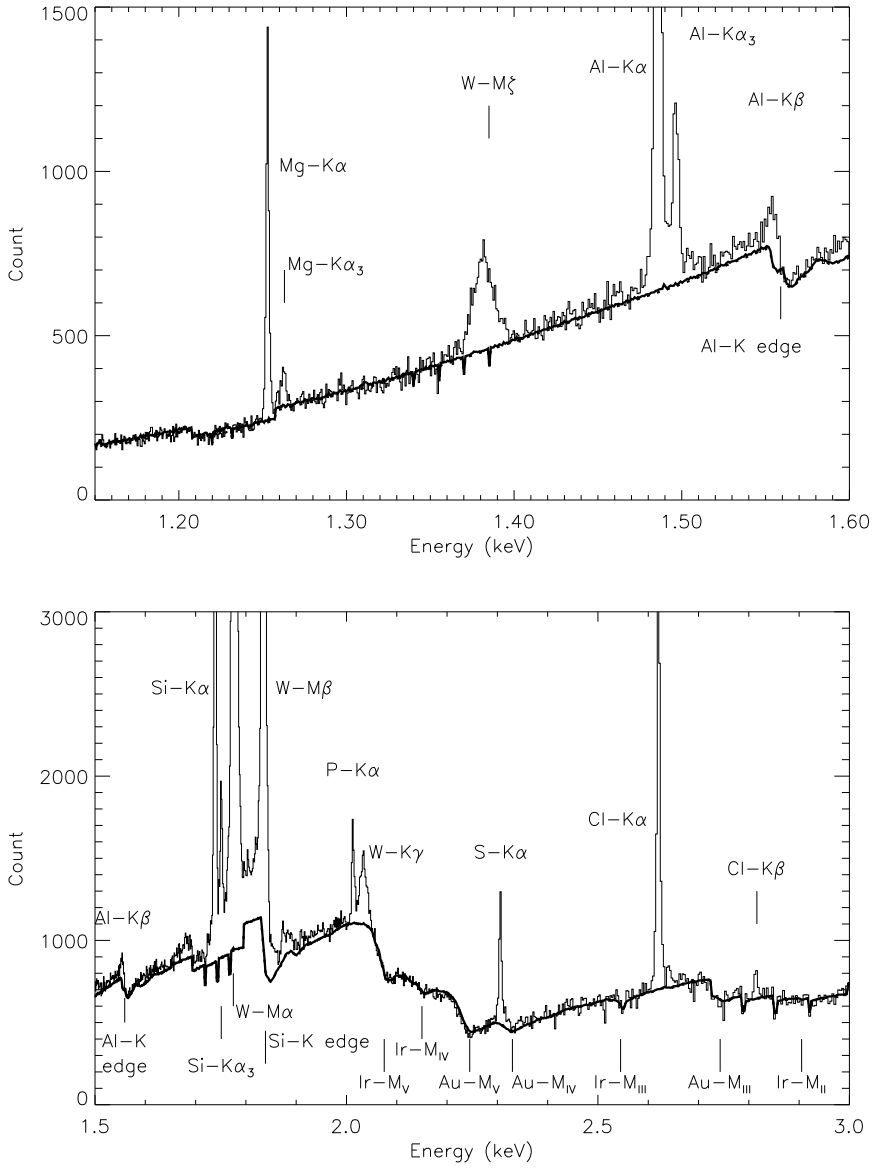

Figure 1: A portion of the calibration spectrum of a carbon source using the HEG portion of the HETGS. Note the emission lines from contaminant elements are quite narrow and are readily identified. The solid line is a model of a 5-parameter model of the source continuum folded with the effective area of the spectrometer and the exposure function.

the ways that Chandra will contribute to the understanding of jets in active galactic nuclei (AGN) and Galactic sources. Briefly, the HETGS consists of two different types of grating facets that tile the annular exit apertures of the telescope mirror shells. The outer mirror pairs focus X-rays through the medium energy gratings (MEG) while the outer pair, with much higher reflectivity at high energies, focusses X-rays through the high energy gratings (HEG). The HEG and MEG spectra are independently measured by the spectroscopic array of ACIS. Canizares et al. (2000) give a somewhat more detailed description.

2 Ground Calibration

In Figure 1, we show ground calibration data that demonstrate the overall performance of the pre-flight HETGS. The HEG portion of the continuum spectrum is well modelled from pre-flight effective areas; the edges near 2.1 keV due to the Ir coating on the mirror and the edges near 2.3 keV due to the Au in the grating do not show residuals after source modelling. The emission lines arise from contaminant elements on the carbon anode in the electron impact source and are readily identified. The spectral resolution of the HETGS is apparent; the narrow K-α lines stand in marked contrast to the broadened W-Mζ and W-Mγ lines at 1.38 and 2.03 keV, respectively.

3 Flight Calibration

The first target observed with Chandra was the quasar PKS 0637–752. It was rather surprising to find an X-ray jet extending 7-12$''$ from the quasar core because the target had been chosen for focus measurements. The core point response function is small enough, however, that the jet had no effect on determining the best detector focus position. New radio observations showed that the radio and X-ray jets were remarkably similar out to 12$''$ where there is a significant bend in the radio emission. The optical fluxes from Hubble data are so low that models of the jet X-ray emission are difficult to develop. See Lovell et al. (2000) for more discussion.

The HETGS flight calibration program includes observations of the Crab Nebula and pulsar in order to verify the absolute effective area of the system, an observations of the late type star Capella in order to verify the spectral resolution with emission lines, and observations of

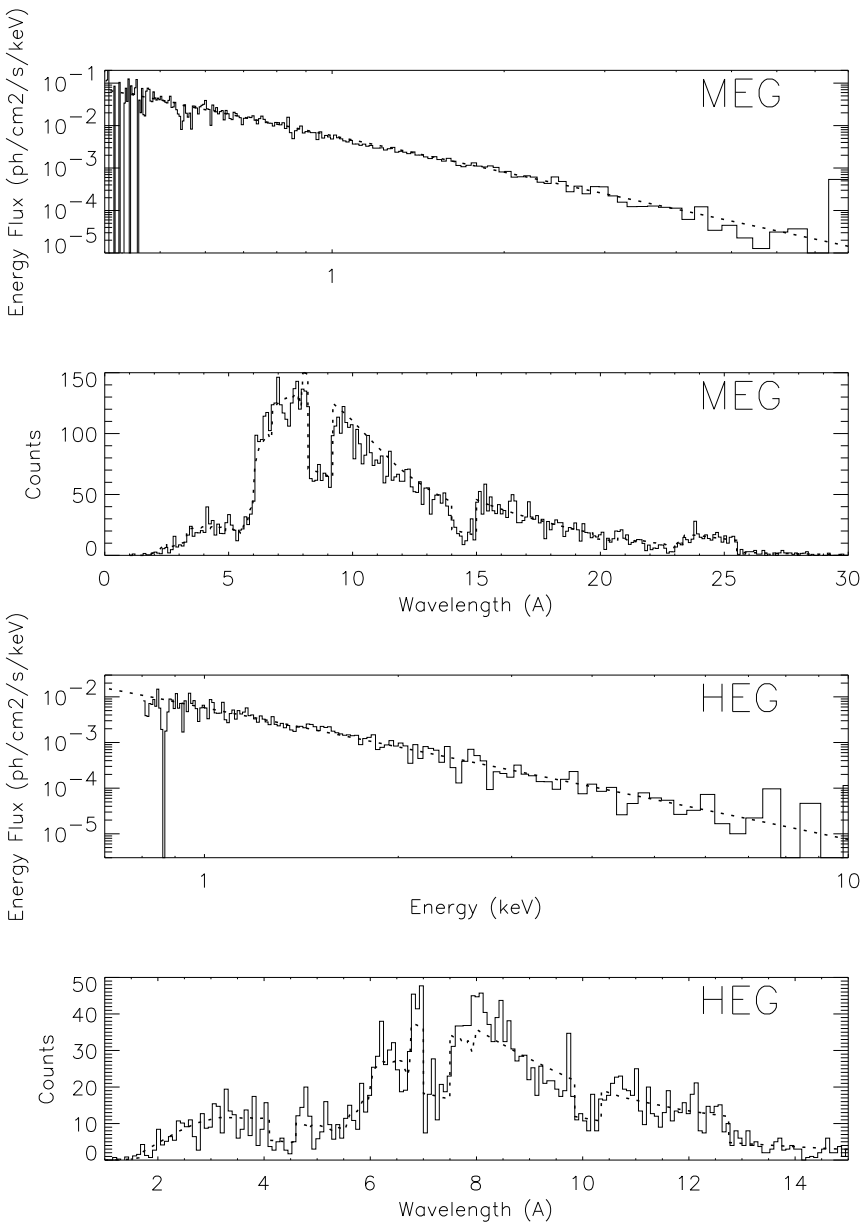

Figure 2: The spectra of Mk 421 with the Chandra HETGS. The top two are the flux and count spectra from the MEG grating data and the bottom two are from the HEG data. The count spectra are overlaid with well-fitting power law models with $\alpha = 1.9$, folded with the instrument effective area and exposure. The MEG and HEG spectra are consistent within 10-20% systematic uncertainties.

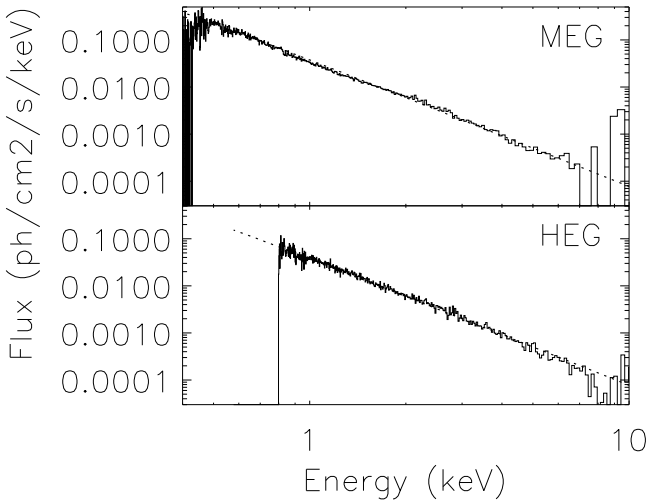

Figure 3: The spectrum of PKS 2155–304 with the Chandra HETGS. As with Mk 421, the MEG and HEG spectra are consistent within 10-20% systematic uncertainties; the spectra are fitted very well by a simple power law $\Gamma = 2.7$.

extragalactic sources 3C 273 and Mk 421 in order to verify the effective area for point sources and cross calibrate with other X-ray spectrometers. The Capella observation (Canizares et al. 2000) shows that the spectral resolution achieved in ground calibration is matched by flight data. The Crab nebula (Weisskopf et al. 2000) shows that the 0th order image reveals significant fine structure that was not previously observed.

4 High Resolution X-Ray Spectra of AGN

The calibration spectra of Mk 421 are shown in Figure 2. The spectra from the MEG and the HEG are consistent with each other within the 10-20% systematic uncertainties. The spectra are well fitted with a simple power law with $\alpha = 1.9$ ($f_\nu \propto \nu^{-\alpha}$) and the only deviation from this fit appears near the O-K edge, which will be removed as the detector calibration is refined.

The BL Lac object PKS 2155–304 was observed as part of the HETGS guaranteed time observation program. Spectra are shown in Figure 3. Again, the HEG and MEG spectra are consistent within 10-20% systematic uncertainties and are well fitted with a simple, pure

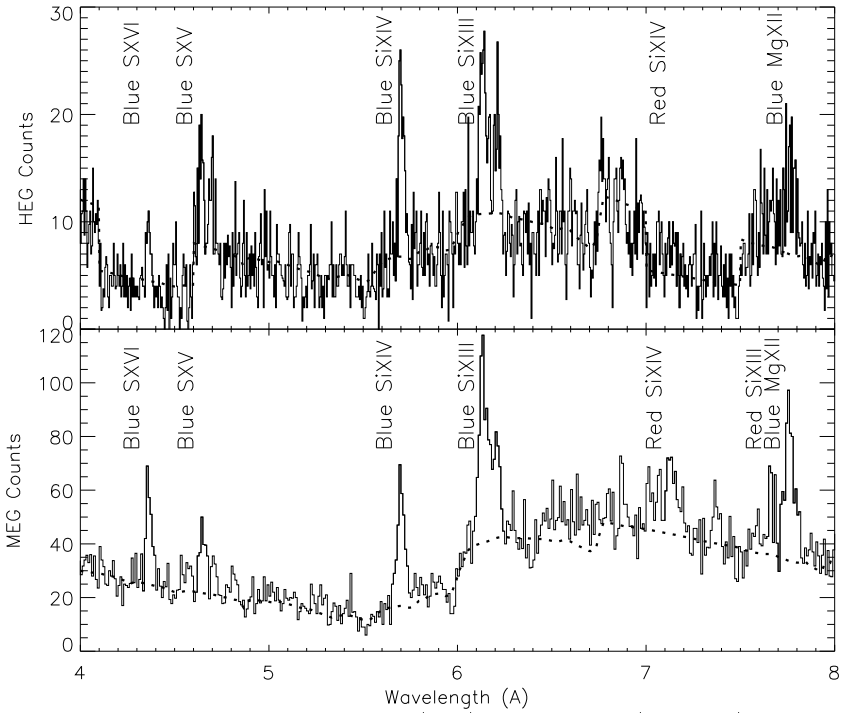

Figure 4: A portion of the HEG (top) and MEG (bottom) spectra of SS 433 observed with the Chandra HETGS, showing the blue-shifted H- and He-like lines of S (S XVI and S XV), the corresponding lines of Si (Si XIV and Si XIII) as well as the red-shifted counterparts to the Si lines. Note that the lines are broadened and that the He-like triplets of S and Si are resolved.

power law model. The spectral index is $1.70 + / - 0.02$ and there are no significant absorption features. A feature such as the one found by Canizares and Kruper (1984) would have been detected easily in the MEG portion of the Chandra HETGS spectrum, so we conclude that it must be variable.

Other AGN observed in the early phase of Chandra HETGS observations include NGC 1275, PKS 2149−305, and Q0836+710. Preliminary analyses indicates that these HETGS spectra are all well fitted by simple power law models with absorption by neutral interstellar material. The spectral indices are somewhat smaller: 0.8, 0.2, and 0.4, respectively. No Fe-Kα lines are detected in any of their spectra.

5 SS 433

The Galactic X-ray binary SS 433 was observed in order to detect and measure X-ray lines from the opposing jets. As shown by Kotani et al. (1996) using ASCA, the blue-shifted lines are so much stronger than the red-shifted lines that Doppler boosting is insufficient to account for the line ratios, so absorption of the red-shifted lines is required. This absorption could arise in the accretion disk. Furthermore, Kotani et al. found that the temperature at the base of the jet must be of order 20 keV in order to give the observed ratio of the Fe XXVI and Fe XXV emission lines.

We observed SS 433 at very nearly the same precessional phase as Kotani et al.; portions of the MEG and HEG spectra are shown in Figure 4. We confirm the result of Kotani et al. that the red lines are systematically weaker than expected but now we can extend this result to the H-like and He-like ions of S and Si; the red-shifted lines are even weaker relative to the blue ones than for the Fe XXV lines. We also find that the lines are broadened significantly, with FWHM values of order 2000-5000 km/s, comparable to the broadening of the optical lines from the jets.

The base of the SS 433 jets, however, must be significantly cooler than found by Kotani et al.. We do not detect either the blue- or the red-shifted Fe XXVI lines at all with a limit that is more than a factor of 5 lower than derived from the ASCA data. The base temperature must be less than 3.5 keV, based on limits to the Fe XXV:Fe XXVI line ratios. We can get additional indications of the jet base temperature using the S XV and S XVI ratio as well as the Si XIII and Si XIV ratio. The S ratio is consistent with emission from a thin thermal plasma with a temperature of $2.3 + / - 0.1$ keV while the Si line ratio gives $1.8 + / - 0.1$ keV. Although these lines can be produced in cooler regions further out in the jet, the limit on the Fe line ratios indicates that the base temperature could be as low as 2.5 keV.

6 Summary

In general, Chandra is working very well and the newest results on AGN and astrophysical jets already promises to change our understanding of these phenomena.

Acknowledgements. I thank the PI of the HETGS, Prof. Claude R. Canizares for his support; Daniel Dewey and other members of the HETGS team with whom I worked during ground calibration; Norbert Schulz, Patrick Ogle, Mike Wise, and other members of the Chandra X-ray Center at MIT who have also contributed to the results presented here. I gratefully thank the VSOP Project, which is led by the Japanese Institute of Space and Astronautical Science in cooperation with many organizations and radio telescopes around the world, for inviting me to participate in this conference. This work was supported by contract SAO SV1-61010.

References

Canizares, C.R. & Kruper, J. 1984, *ApJ*, **278**, L99

Canizares, C.R., Huenemoerder, D.P., Davis, D.S., et al., 2000, in preparation

Kotani, T., Kawai, N., Matsuoka, M., & Brinkmann, W. 1996, *PASJ*, **48**, 619

Lovell, J.E.J., Tingay S.J., Piner, B.G., et al. 2000, *these Proceedings*

Weisskopf, M., Hester, J.J., Tennant, A., et al., 2000, in preparation